EFFECTS OF THE SOLAR WIND CONDITIONS ON THE GLOBAL MAGNETOSPHERIC CONFIGURATION AS DEDUCED FROM DATA-BASED FIELD MODELS

N.A. Tsyganenko

Hughes STX Corporation, NASA GSFC, Greenbelt, MD 20771, U.S.A.

ABSTRACT

This paper describes results of data-based modeling of the magnetospheric configuration and its response to changes in the solar wind dynamical pressure and the IMF. Previous models did not have a pre-defined magnetopause, they were calibrated by the Kp-index only, and thus did not allow proper modeling of solar wind effects. The new models explicitly include (i) the solar-wind-controlled magnetopause, (ii) Region 1 and 2 Birkeland currents, and (iii) the interconnection of the magnetospheric and solar wind fields at the boundary. They predict the most significant effects of solar wind variations upon the global magnetospheric structure. On the dayside, the Region 1 Birkeland currents cause major changes of the magnetic configuration, as the IMF turns southward. The tail current intensity is controlled mainly by the pressure of the solar wind, although the influence of the southward IMF is also clearly seen. The effects of the IMF-induced interconnection field were found to be quite significant.

1. INTRODUCTION

Unlike the main geomagnetic field on the Earth's surface, the distant magnetospheric field varies constantly in response to changes in the solar wind conditions, such as the ram flow pressure and the transverse component of the IMF. Quantitative magnetospheric models should be able to replicate at least gross features of those dynamics, associated with the global compression of the magnetopause and the buildup/decay of major current systems. The existing data-based models [Mead and Fairfield, 1975; Tsyganenko and Usmanov, 1982; Tsyganenko, 1987, 1989, referred henceforth as MF75, TU82, T87, and T89, resp.], though used in many studies, did not directly relate the magnetospheric configurations to the parameters of the solar wind. Another problem of those models was their inability to explicitly prescribe the location of the magnetopause as a function of the solar wind state and to quantitatively describe the interconnection between the Earth's magnetic field and the IMF.

In recent years, significant progress was made in the development of new-generation magnetospheric models, based on large sets of spacecraft data, which allowed for the first time the tracing of global effects of the solar wind on the observed geomagnetic field configurations.

This paper briefly describes the principles of constructing the new model and discusses the most important effects of solar wind conditions upon the model field structure.

2. OVERVIEW OF THE APPROACH

The modeling region extends from low altitudes up to the distant geotail, practically all of near-Earth space surveyed by magnetometer-carrying spacecraft. In the data-based models developed during the last decade (T87, T89), the modeling region ended at the lunar distance, since the most distant portion of the data was provided by the Moon-orbiting spacecraft Explorer-35.

The data for the present modeling study came from 11 spacecraft, covering the period from 1966 to 1986 [Fairfield et al., 1994]. The vector field data were edited, averaged over 10-25 min intervals, and tagged by the corresponding values of the hourly average solar wind parameters and the geomagnetic activity indices. Although the total number of the field averages in the cumulative database amounted to 79,745, this study used only the 46,759 for which both IMF and solar wind plasma parameters were known.

The representation of the magnetic field in the modeling region is based on the modular principle, according to which the external part of the total field $\vec{\mathbf{B}}_E$ is represented as the sum of contributions from all major magnetospheric current systems

$$\vec{\mathbf{B}}_E = \vec{\mathbf{B}}_{MP} + \vec{\mathbf{B}}_{RC} + \vec{\mathbf{B}}_T + \vec{\mathbf{B}}_{R1} + \vec{\mathbf{B}}_{R2} + \vec{\mathbf{B}}_{Int} \quad (1)$$

The terms on the righthand side correspond, respectively, to the magnetopause current system, the ring current, the tail current sheet, the Region 1 and 2 Birkeland current systems, and the interconnection term due to partial penetration of the IMF into the magnetosphere. Each term in (1) was parametrized by its own set of input indices/parameters, and the net model field was fitted by least squares to the entire set of data, deriving the regression coefficients which define the amplitudes of response of the individual currents to the input parameters.

An important novel feature of the present approach is the way of parametrizing the model. In all previous modeling studies, the whole dataset was divided into several subsets, corresponding to different intervals of the Kp-index, and then separate sets of model coefficients for each Kp-interval were found. However, in the case of more than one input parameter, this approach becomes unfeasible due to rapidly growing number of bins in the multi-dimensional parameter space and, hence, too few data points in the individual subsets.

In the present model, the input parameters (like solar wind pressure, Dst, etc.), denoted here as $\{a_1, a_2, ..., a_N\}$, enter the field components as continuous variables and, therefore, are treated in the same way as the spatial coordinates $\{x, y, z\}$ and the geodipole tilt angle Ψ. This means that the components of the model field vector $\vec{\mathbf{B}}$ are actually considered as functions

Proc. Third International Conference on Substorms (ICS-3), Versailles, France, 12 – 17 May 1996, ESA SP-389 (October 1996)

of position in the space $\{x, y, z, \Psi, a_1, a_2, ..., a_N\}$ with the dimensionality $N + 4$.

Another aspect of least-squares fitting of the model field to data is the choice of the merit finction. In the earlier models, the minimized quantity was the r.m.s. deviation of the full vectors of the model field from the corresponding measured vectors. Due to several factors, discussed in detail in [Tsyganenko, 1995], this choice resulted in unstable distributions of the weak equatorial B_z on the nightside. In the new models, we adopt a "mapping-oriented" fitting criterion, in which the merit function is based on the r.m.s. difference of the unit direction vectors $\mathbf{b} = \mathbf{B}/B$ between the model and observations, which results in more robust and realistic configurations.

3. MODELING INDIVIDUAL CURRENT SYSTEMS

In this section, a more detailed discussion of the major model field sources is given.

3.1. The Magnetopause Magnetic Field

The term $\vec{\mathbf{B}}_{MP}$ represents the field responsible for confining the field of all internal magnetospheric sources within the model boundary. In previous data-based models, the magnetopause field was represented by simple analytical functions of a general form, whose coefficients were fitted to the observed field. However, since those models did not use any information on the actual position of the magnetospheric boundary, the model magnetopause appeared as a de-facto surface separating the field lines connected to Earth from those draping the magnetosphere from outside. Although the position of this separatrix boundary appeared to be in a fair agreement with the observed magnetopause on the dayside, its shape in the tail region often significantly differed from the expected one and could not be easily controlled by the representations used.

In the newly devised models, the position and shape of the magnetopause is explicitly defined as an analytical surface: a half-ellipsoid sunward from the lunar distance, smoothly continued by a cylinder down the far tail. The shape and size of this boundary are similar to those deduced from direct observations of the magnetopause crossings by Sibeck et al. [1991], and assume a self-similar expansion/contraction of the boundary in response to variations of the solar wind pressure.

As soon as the position of the model magnetopause is known, the field of the magnetopause currents can be found for any distribution of internal magnetospheric field sources, by using an appropriate combination of scalar potentials with a sufficient degree of flexibility. By varying the free parameters which describe those potentials, one can find a best-fit solution which minimizes the r.m.s. normal component of the total field over the boundary of the modeling region [Schulz and McNab, 1987, 1996; Tsyganenko, 1995]. Such a "shielding" field can be found separately for each term in (1), and $\vec{\mathbf{B}}_{MP}$ is the sum of all such fields. This method allows to independently change the intensities of the individual sources, keeping the net field confined within the magnetopause for any combination.

Another advantage of the above method is that the magnetopause field can be approximated by a relatively simple combination of analytical functions, allowing fast computation of the field components. That feature is important for many applications, such as the tracing of a large number of field lines or massive calculations of charged particle orbits.

In the present version of the model, the only parameter that controls the size of the magnetopause is the solar wind ram pressure. It was assumed that under average solar wind conditions with the pressure $\langle p_{dyn} \rangle = 2\,nPa$, the size and shape of the boundary is close to the one found by Sibeck et al. [1991], with the subsolar distance $R_S \approx 11.0 R_E$, the dawn-dusk radius $R_D \approx 15.0 R_E$, and the asymptotic tail radius (near Moon's orbit) $R_M \approx 28.2 R_E$. It was further assumed that variations of the pressure around its average value cause self-similar compression/expansion of the boundary with a uniform spatial scaling of all field sources, $\vec{\mathbf{r}} \rightarrow \kappa \vec{\mathbf{r}}$, where $\kappa = \left(p_{dyn}/\langle p_{dyn} \rangle\right)^{\alpha}$. In the simplest case with no field sources inside the magnetosphere other than the Earth's dipole, the parameter α equals $1/6$ [Mead and Beard, 1964]. In the actual magnetosphere, however, the use of the above scaling law is at best an approximation, and for that reason α it was considered a free model parameter, fitted to data together with other parameters. Its best-fit value was found to be $\alpha \approx 0.14$, close to the above theoretical estimate.

Although it is established that the magnetopause shape also depends on the interplanetary field orientation [Petrinec and Russell, 1993], in this model the role of the IMF is limited to parametrizing the intensities of the tail and Region 1 Birkeland currents, and to controlling the effect of partial penetration of the IMF inside the magnetosphere.

3.2. The ring/tail currents

The ring current field representation in this model was based on the approach used by the TU82/T89 models [Tsyganenko and Peredo, 1994]. More specifically, the model is based on a simple vector potential representation for an axially symmetric field, corresponding to a spread-out near-equatorial distribution of the electric current. Several vector potentials were superposed, with appropriate weights and spatial scale sizes, a day-night asymmetry was introduced, as were a finite thickness which could be varied in the X- and Y-directions, a shift along the Sun-Earth line, and effects of the geodipole tilt (two-dimensional warping). All this produced flexible and compact representations, which proved to be quite effective "building blocks" for both the ring current and the tail current sheet models [Tsyganenko, 1995].

The principal difference between the ring and tail current is that, due to much larger spatial extent of the latter, the tail current crosses the magnetopause, and hence adding its shielding field removes from the model all contributions from the part of the current flowing outside the magnetopause, replacing it with the contribution from the tail closure current flowing on the magnetopause itself. However, from the mathematical point of view that circumstance does not pose any problem, and the algorithm for obtaining the shielding field is the same for both modules [Sotirelis et al., 1994].

Another aspect of ring/tail current modeling is that the electric current distribution should be flexible enough to represent a wide variety of possible day-night and dawn-dusk profiles of current density. This is achieved by combining two or three "modes" with different variation scale sizes and variable weight coefficients. These coefficients, in turn, are represented as simple functions of relevant model input parameters.

The ring current magnitude was parametrized by a composite "RC-index", which is essentially the Dst-index, corrected for the effect of a varying solar wind pressure whose value in nanopascals is $p_{dyn} = 1.94 \cdot 10^{-6} N V_{sw}^2$. More specifically, the ring current amplitude was assumed to vary linearly as $a_1 + b_1 RC$, where

$$RC = k_1 Dst - k_2 \sqrt{p_{dyn}}\,. \qquad (2)$$

The coefficient k_1 multiplying the Dst-index is a correction factor for the effect of the geomagnetically induced currents inside Earth, and was assumed equal to 0.8; the second coefficient, k_2, was set equal to 13, derived from pressure balance at the subsolar point and from the shielding factor for the adopted magnetopause shape.

The amplitudes of the tail modes were assumed as linear forms

$$a_i + b_i \left(\sqrt{p_{dyn}/\langle p_{dyn}\rangle} - 1\right) + c_i \left(\gamma/\langle\gamma\rangle - 1\right) \quad (3)$$

depending on the solar wind pressure p_{dyn} and on the parameter

$$\gamma = N^{1/2} V_{sw} \left(B_y^2 + B_z^2\right)^{1/2} \sin(\theta/2) \quad (4)$$

depending on the transverse component (y, z) of the IMF and its angle θ relative to the GSM north direction [Iijima and Potemra [1982]]. The same index γ was used for parametrizing the Region 1 Birkeland current system, as discussed below. In the preliminary version of the model, discussed in this paper, two tail modes were included in the term $\vec{\mathbf{B}}_T$, so that the total number of ring/tail current free parameters was 8.

3.3. Modeling Birkeland current systems

The large-scale systems of Birkeland currents is a novel feature of this data-based magnetospheric field model; the details of the approach are described by Tsyganenko and Stern, [1996]. All previous models did not attempt to explicitly include this important element, although the role of the Region 1 Birkeland currents in the dynamics of the dayside magnetospheric configurations was conjectured long ago [e.g., Maltsev and Lyatsky, 1975].

Earlier global models, which assumed distributed currents inside the magnetosphere, other than the tail and ring currents (MF75, TU82, T87, T89), as well as a separate modeling study of the dayside magnetic field structure [Tsyganenko and Usmanov, 1984], revealed a persistent equatorward shift of the polar cusps with growing disturbance level, which could not be entirely attributed to the tail/ring current effects, and therefore had to be explained as due to the field from the Region 1 field-aligned currens. Later studies [Donovan, 1993; Tsyganenko and Sibeck, 1994] confirmed that the global magnetic effects of Birkeland currents are quite significant.

In the new model, the field from the Region 1 and 2 Birkeland current systems is explicitly represented, based on existing information on their configuration above the ionosphere and at larger distances. The formalism of Euler potentials provided the basis for the mathematical representation of the Birkeland current sheets, using a simple coordinate system, in which the flow lines of the electric current vector

$$\vec{\mathbf{j}} = \nabla\xi \times \nabla\chi \quad (5)$$

reside on the coordinate surfaces ξ =constant and have a geometry, close to the expected one. The distribution of the current strength along the ionospheric Region 1 and 2 ovals was specified in accordance with the statistical results of Iijima and Potemra [1976]. The magnetic field produced by the model electric current systems was computed at a large set of points within the modeling region by means of Biot-Savart integration and was then approximated by simple analytical forms. At low altitudes, the resulting distribution of the model magnetic field due to Region 1 and 2 field-aligned currents resembles typical profiles observed by polar-orbiting spacecraft [e.g., Zanetti et al., 1983].

As with any other module contributing to the net model field, the terms for the Birkeland field should be parametrized by appropriate indices and/or solar wind parameters and then fitted to data. In this version of the model, the Region 1 current amplitude was represented as a linear function of the parameter γ, given by (4) and used for parametrizing the tail field as well. As shown by Iijima and Potemra [1982], the parameter γ has the largest correlation with the density of the Region 1 field-aligned current measured at ionospheric altitudes.

The model field of the Region 2 current was parametrized as a linear function of the AE-index, based on the assumption that the principal source for the partial ring current and associated Region 2 currents is the storm-time injection of fresh particles on the nightside.

3.4. The interconnection magnetic field

Already in the early days of the magnetospheric physics [Dungey, 1961] it was predicted that the existence of an interplanetary magnetic field makes the magnetosphere open. The interconnection between the solar wind magnetic field and the geomagnetic field was theoretically introduced in several quantitative models, from the crude case of a constant field added to a purely dipolar field [Stern, 1973], to quite sophisticated models [e.g., Toffoletto and Hill, 1993]. However, no attempt has been done so far to directly derive the average interconnection field from a large set of the magnetospheric field measurements, combined with simultaneous IMF data.

In this data-based modeling study, the interconnection field is introduced as a separate component in the sum (1). Its orientation is controlled by B_y and B_z in the solar wind and its amplitude is derived by fitting the total model field to the whole body of the magnetospheric field measurements.

In more detail, the interconnection field at the boundary was assumed to contribute there a non-zero normal component

$$B_n = \vec{\mathbf{B}}_{MS} \cdot \vec{\mathbf{n}} \quad (6)$$

where $\vec{\mathbf{n}}$ is the outward unit normal vector and $\vec{\mathbf{B}}_{MS}$ is the magnetosheath field in the immediate vicinity of the magnetopause. That field was assumed, for simplicity, to have only y- and z-components, proportional to the IMF B_y and B_z:

$$\vec{\mathbf{B}}_{MS} = kP(x)Q(y')(\vec{\mathbf{B}}_y + \vec{\mathbf{B}}_z) \quad (7)$$

The functions $P(x)$ and $Q(y')$ in the righthand side approximate, respectively, the variation of the interconnection efficiency with the distance from the subsolar region along the X_{GSM}-axis, and its variation vs the distance from the plane containing the Sun-Earth line and the IMF vector. The simplest case of $P(x) = Q(y') = 1$ corresponds to a uniform field in the magnetosheath, which gives rise to a uniform penetrating field. However, it is more likely that the interconnection is concentrated near the subsolar point and decreases tailward [Toffoletto and Hill, 1989]. Similarly, with regard to the coordinate y', the normal component is likely to be largest near the plane $y' = 0$, where the IMF transverse component is nearly normal to the tail boundary [Pudovkin and Semenov, 1985]. For that reason, the functions P and Q in (7) were assumed to have the general form

$$\begin{aligned} P(x) &= \exp(x/\Delta X) \\ Q(y') &= \exp\left[-(y'/\Delta Y)^2\right] \end{aligned} \quad (8)$$

The interconnection field deeper inside the magnetosphere should be expressible by a scalar potential and its normal

component must fit B_n of (6); in other words, it should be sought as a harmonic solution of the boundary value problem. In this model, the scalar potential was specified as a superposition of the "box" harmonics [Tsyganenko, 1995]

$$U_{i,k} \sim \exp\left[\sqrt{\frac{1}{p_i^2}+\frac{1}{p_k^2}}\,x\right]\cos\frac{y}{p_i}\sin\frac{z}{p_k} \qquad (9)$$

whose coefficients were fitted to obtain the closest matching of the normal component on the boundary, $-\nabla U \cdot \vec{\mathbf{n}}$, to that given by (6)-(8). After that, the value of the penetration factor k in (7) was found by fitting the entire model field (1), with the interconnection term $\vec{\mathbf{B}}_{Int} = -\nabla U$, to the entire set of spacecraft data, using the observed values of the IMF components for parametrizing the interconnection field.

4. RESULTS

4.1. Amplitudes of individual sources as functions of the model input

The behavior of most field components in the new model was found to be in reasonable agreement with expectations.

(1) The Region 1 coefficients indicate a strong dependence on the index γ, so that for $B_z = -5\,nT$, $N = 10\,cm^{-3}$, and $V_{sw} = 500\,km/s$, the total current amounts to $1.3MA$, causing significant changes in the dayside magnetic configuration. During periods with northward IMF, the current drops down to nearly zero.

(2) The total Region 2 current was found to be $\sim$ $1MA$, in a rough agreement with the estimates of Iijima and Potemra [1976]. However, practically no dependence on the AE-index was inferred, and the most plausible explanation is that the number of data points in the relevant regions ($R \sim 5-7R_E$ in the nightside equatorial magnetosphere) was too low for resolving gross features of the partial ring current dependence on the disturbance level.

(3) The tail mode coefficients show a strong dependence on the solar wind pressure and a relatively weaker response to the parameter γ, especially for the longer tail mode.

(4) A relatively large regression coefficient with the RC-index (2) was obtained for ring current. However, its total magnitude was found to be significantly less than expected; the most likely reason is the lack of data in the ring current region which may also have affected the modeled Region 2 current. An interplay between these two terms is quite possible.

(5) The magnetopause field, as mentioned above, was assumed to be controlled by the solar wind pressure only, and the best-fit value of the parameter κ in the scaling law was found equal to 0.14, close to the theoretical estimate [Mead and Beard, 1964].

(6) The value of the parameter k in equation (7) was found equal to 0.81, which means that the interconnection effect is quite strong and can be detected with a sufficient confidence by using the methods of data-based modeling.

4.2. Model field configurations

Figure 1 shows an example of the model field line configuration for the conditions on June 30, 1988, when a strong southward

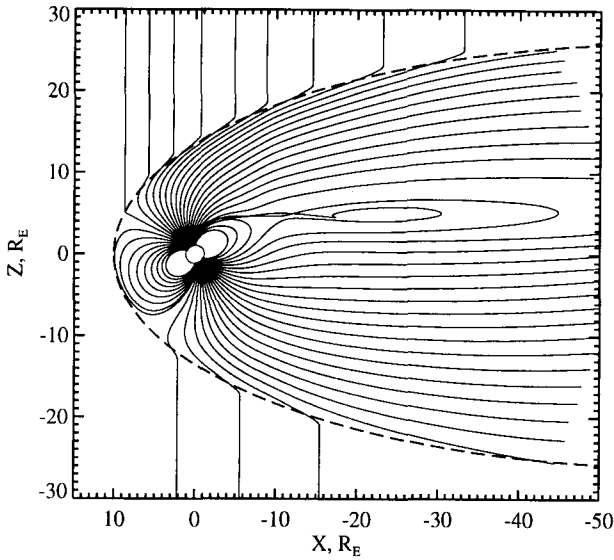

Figure 1: The noon-midnight projection of the model field lines for the solar wind conditions of June 30, 1988, with p_{dyn} =3.7 nPa, IMF B_y =-0.7 nT and B_z = -6.8 nT. The apparent crossing of the field lines in the plasma sheet as well as a wiggle on one of the lines at $X \approx -15R_E$ is a projection effect caused by formation of a three-dimensional loop due to finite Y-component of the IMF.

IMF ($B_z = -6.8\,nT$) was combined with enhanced solar wind pressure ($p_{dyn} = 3.7\,nPa$). According to the model, the total Region 1 Birkeland current in this event could have reached $1.5MA$, and caused a significant equatorward shift of the polar cusps (though somewhat masked by a large dipole tilt angle) and a depressed field in the subsolar region. It is interesting, however, that this estimate is well below the value of the net Region 1 current according to Bythrow and Potemra [1983]: for the same solar wind conditions with the merging electric field $E = 3.5\,mV/m$, their Figure 4 gives $I_{tot} = 6MA$. Increasing the model Region 1 current up to this value would result in an enormous restructuring of the magnetospheric field on both the day and night sides, indicating that the result of Bythrow and Potemra [1983] probably overestimates the actual current.

Figure 2 displays a configuration for the opposite case with a strongly northward IMF. Note that the field line geometry outside the magnetopause in both cases is based solely on the approximation (7) and, hence, does not represent the actual average magnetosheath field, which drapes around the boundary and therefore has a significant B_x-component. To obtain a realistic geometry of this draping, one needs to model the magnetosheath as well, which goes beyond the scope of the present study.

5. CONCLUSIONS

A new approach to data-based modeling of the magnetospheric magnetic configuration has been developed and successfully implemented. The new models are parametrically controlled by the solar wind pressure, the transverse components of the IMF, and by indices of the geomagnetic activity. In contrast to previous data-based representations, the new models have an explicit magnetopause whose size varies in response to changes of the solar wind pressure, and it also includes an IMF-controlled interconnection of the geomagnetic and solar wind magnetic fields across the boundary. An important novel element of the model is the separate representation of the field

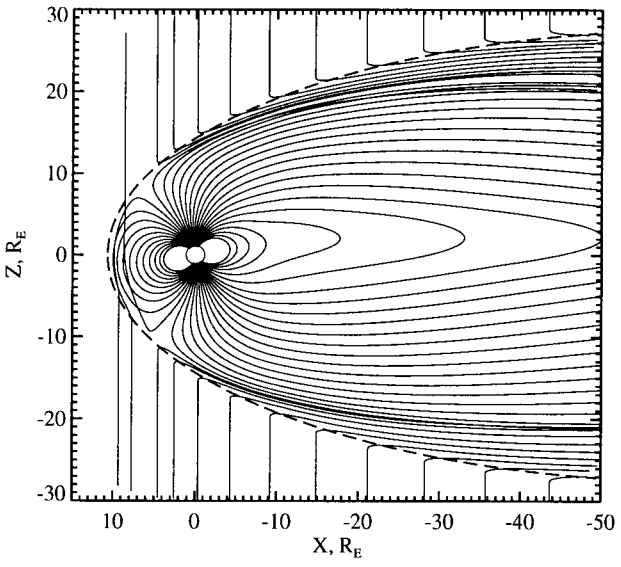

Figure 2: The noon-midnight projection of the model field lines for the solar wind conditions of June 13, 1988, with p_{dyn} =2.5 nPa, IMF B_y =4.0 nT and B_z =+10.7 nT. The strongly northward IMF with a significant dawn-dusk component results in the tail-lobe reconnection geometry and much less stretched equatorial tail lines, in comparison with Fig.1.

from the large-scale systems of Birkeland currents. The model provides realistic and robust magnetic configurations for specific combinations of input parameters. In particular, the modeling results confirm that the Region 1 field-aligned currents play crucial role in the restructuring of the dayside magnetic field during the periods with the southward IMF orientation.

ACKNOWLEDGMENTS

The author thanks David Stern for his constructive comments on the manuscript. This work is supported by NASA grant NAS5-32350 and NSF Magnetospheric Physics Program grant ATM-9501463.

REFERENCES

Bythrow, P.F. and T.A. Potemra, The relationship of total Birkeland currents to the merging electric field, *Geophys.Res.Lett., 10,* 573-576, 1983.

Donovan, E.F., Modeling the magnetic effects of field-aligned currents, *J.Geophys. Res., 98,* 13,529-13,543, 1993.

Dungey, J.W., Interplanetary magnetic field and the auroral zones, *Phys.Rev.Lett., 6,* 47-48, 1961.

Fairfield, D.H., N.A. Tsyganenko, A.V. Usmanov, and M.V. Malkov, A large magnetosphere magnetic field database, *J.Geophys.Res., 99,* 11319-11326, 1994.

Iijima, T. and T.A. Potemra, The amplitude distribution of field-aligned currents at northern high latitudes observed by Triad, *J.Geophys.Res., 81,* 2165-2174, 1976.

Iijima, T. and T.A. Potemra, The relationship between interplanetary quantities and Birkeland current densities, *Geophys.Res.Lett., 9,* 442-445, 1982.

Maltsev, Yu.P. and W.B. Lyatsky, Field aligned currents and erosion of the dayside magnetosphere, *Planet. Space Sci., 23,* 1257-1260, 1975.

Mead, G.D. and D.B. Beard, Shape of the geomagnetic field solar wind boundary, *J.Geophys.Res., 69,* 1169-1179, 1964.

Mead, G.D. and D.H. Fairfield, A quantitative magnetospheric model derived from spacecraft magnetometer data, *J.Geophys.Res., 80,* 523-534, 1975.

Petrinec, S.M., and C.T. Russell, An empirical model of the size and shape of the near-Earth magnetotail, *Geophys.Res.Lett., 20,* 2695-2698, 1993.

Pudovkin, M.I., and V.S. Semenov, Magnetic field reconnection theory and the solar wind-magnetosphere interaction: A review, *Space Sci.Rev., 41,* 1-89, 1993.

Schulz, M., and M. McNab, Source-surface model of the magnetosphere, *Geophys.Res.Lett., 14,* 182, 1987.

Schulz, M., and M. McNab, Source-surface modeling of planetary magnetospheres, *J.Geophys.Res., 101,* 5095-5118, 1996.

Sibeck, D.G., R.E. Lopez, and E.C. Roelof, Solar wind control of the magnetopause shape, location, and motion, *J.Geophys.Res., 96,* 5489-5495, 1991.

Sotirelis, T., N.A. Tsyganenko , and D.P. Stern, Method for confining the magnetic field of the cross-tail current inside the magnetopause, *J.Geophys.Res., 99,* 19393-19402, 1994.

Stern, D.P., A study of the electric field in an open magnetosphere, *J.Geophys.Res., 78,* 7292-7305, 1973.

Toffoletto, F.R. and T.W. Hill, Mapping of the solar wind electric field to the Earth's polar caps, *J.Geophys. Res., 94,* 329-347, 1989.

Toffoletto, F.R. and T.W. Hill, A nonsingular model of the open magnetosphere, *J.Geophys. Res., 98,* 1339-1344, 1993.

Tsyganenko, N.A. and A.V. Usmanov, Determination of the magnetospheric current system parameters and development of experimental geomagnetic field models based on data from IMP and HEOS satellites, *Planet. Space Sci., 30,* 985-998, 1982.

Tsyganenko, N.A. and A.V. Usmanov, Effects of the dayside field-aligned currents in location and structure of polar cusps, *Planet. Space Sci., 32,* 97-105, 1984.

Tsyganenko, N.A., Global quantitative models of the geomagnetic field in the cislunar magnetosphere for different disturbance levels, *Planet. Space Sci., 35,* 1347-1358, 1987.

Tsyganenko, N.A., A magnetospheric magnetic field model with a warped tail current sheet, *Planet. Space Sci., 37,* 5-20, 1989.

Tsyganenko, N.A., and M. Peredo, Analytical models of the magnetic field of disk-shaped current sheets, *J.Geophys.Res., 99,* 199, 1994.

Tsyganenko, N.A., and D.P. Stern, Modeling the global magnetic field of the large-scale Birkeland current systems, submitted to *J.Geophys.Res.*, 1996.

Tsyganenko, N.A., Modeling the Earth's magnetospheric magnetic field confined within a realistic magnetopause, *J.Geophys.Res., 100,* 5599-5612, 1995.

Tsyganenko, N.A. and D.G. Sibeck, Concerning flux erosion from the dayside magnetosphere, *J.Geophys.Res., 99,* 13,425-13,436, 1994.

Zanetti, L.J., W. Baumjohann, and T.A. Potemra, Ionospheric and Birkeland current distributions inferred from the MAGSAT magnetometer data, , *J.Geophys.Res., 88,* 4875-4884, 1983.